

Supporting Information

Instantaneous gelation of a new copper(II) metallogel amenable to encapsulation of a luminescent lanthanide cluster

*William J. Gee^a and Stuart R. Batten^{*a}*

^a School of Chemistry, Monash University, Clayton, Melbourne, Vic 3800, Australia.

Fax: +61 (0)3 99054597; Tel: +61 (0)3 99054505 E-mail:stuart.batten@monash.edu

S1	Synthetic protocols	p2
S1.1	General	p2
S1.2	Typical methodology for gel synthesis	p2
S1.3	Gelation tests whereby gel components were varied	p3
S1.4	Synthesis of europium containing metallogel	p4
S2	Crystallographic data	p5
S2.1	Crystallographic data for [CuCl ₂ (Hppy) ₂]	p5
S2.2	Selected bond lengths and angles for [CuCl ₂ (Hppy) ₂]	p5
S3	Cu(ClO ₄) ₂ gel	p7
S3.1	SEM image of Cu(ClO ₄) ₂ gel	p7
S4	Spectroscopic data	p8
S4.1	Solution IR spectra of ligand, ligand + metal chloride and metallogel	p9
S4.2	Raman spectrum of metallogel and metallogel containing 1	p10
S5	Powder XRD data and discussion	p11
S6	Titration Curve of Hppy with triethylamine	p12
S7	References	p13

S1. Synthetic protocols:

S1.1. General: All chemicals were purchased from Sigma-Aldrich and were used as received. The ligand **Hppy** was synthesized according to a literature procedure.^{S1} Electrospray ionization spectra were recorded on a *Micromass* Platform II QMS spectrometer. Solid-state IR spectra were recorded on a Bruker Equinox 55 Infrared Spectrometer fitted with a Specac Diamond ATR source. Solution RTIR scanning measurements were recorded using a Mettler Toledo ReactIR 10 spectrometer fitted with a DiComp probe and connected to an MCT detector by a K6 Conduit. Scanning was performed in the region of 4000–650 wavenumbers at 8 wavenumber resolution. Elucidation of reaction components was performed using ConcIRTTM software. Raman spectroscopy was performed with either a Renishaw RM2000 spectrometer fitted with a 782 nm Renishaw diode laser or a Renishaw Invia spectrometer fitted with a 514 nm argon ion laser. Scanning electron microscope (SEM) images were collected using a JEOL 7001F field emission gun SEM, operating at an accelerating voltage of 10.0 kV and working distance of 10.0 mm. The gels were dried at room temperature on a silicon chip, and coated with a platinum conductive coating prior to analysis.

S1.2. Typical methodology for metallogel synthesis: Instantaneous gellation was observed by mixing copper(II) chloride (42 mg, 0.31 mmol) in 1 mL DMF with a solution of **Hppy** (50 mg, 0.34 mmol) and triethylamine (34 mg, 0.46 mmol) in DMF (2 - 15 mL). IR (ReactIR): ν_{max} 3557m, 1676m, 1649s, 1618m, 1525w, 1438m, 1393m, 1362m, 1226m, 1101m, 1023m, 845m, 798m, 712m. Raman: 1619, 1535,

1450, 1317, 1222, 1190, 1028, 952, 710, 667, 225. MS (ESI) m/z : 239.2
[Cu(ppy)⁺+MeOH]⁺, 353 [Cu(ppy)₂+H]⁺.

S1.3. Gelation tests whereby gel components were varied: When a DMF solution of **Hppy** reacted with various salts of copper(II), various transition metal chlorides and copper(II) in varied solvents. Gelation properties are summarised in Table S1.

Table S1 Observed gelation properties

Entry	TM(II) salt ^a	Observation	Entry	Solvent	Observation
1	Mn	P	10	EtOH	P
2	Fe	P	11	MeOH	P
3	Co	P	12	CHCl ₃	P
4	Ni	S ^b	13	CH ₂ Cl ₂	P
5	Zn	P	14	Et ₂ O	I
Entry	Cu(II) anion	Observation	15	THF	P
6	SO ₄	P	16	Pyridine	P
7	ClO ₄	G	17	H ₂ O	S ^b
8	Br	P	18	Hexane	I
9	Ac	P			

^a TM = transition metal chloride salt. ^b solutions were found to persist after 7 days time. P = precipitate, S = solution, G = steady gel, I = ligand insoluble.

Copper(II) chloride was exchanged for other divalent transition metal chlorides (M = Mn, Fe, Co, Ni, Zn) which resulted in the formation of precipitates, with the exception of nickel, where the complex remained in solution even at high weight percentages. This is attributed to the affinity of nickel to square planar geometries, coupled with diminished Jahn-Teller distortion relative to copper. Hence Cu and Ni yield square planar complexes, yet only Cu forms the long, weak M-Cl interactions necessary to assemble the complexes into chains. Replacing the chloride anion with

common counteranions (SO_4 , ClO_4 , Br , Ac) also typically yielded precipitates in place of the gel, with the exception of perchlorate, which at the higher wt% of 6.25% yielded a metallogel. SEM analysis of the perchlorate gel determined the nano-fibres to possess a tape-like morphology (See S3.1) that was found to degrade rapidly under the electron beam. Gelation was also found to be limited to the solvent DMF, with water completely dissolving the copper complex and less polar protic and aprotic solvents (EtOH , MeOH , CHCl_3 , CH_2Cl_2 , Et_2O , THF, pyridine) yielding precipitates. Additionally, the behaviour of a preformed DMF gel was evaluated in various solvents and found to dissolve in water, exhibit immiscibility in hexane and partial immiscibility in the above listed protic and aprotic solvents (attributed to uptake of DMF from the gel pores into the solution).

S1.4. Synthesis of europium containing metallogel: The gel containing europium cluster **1** was synthesised by the sequential addition of 1 mL DMF solutions containing copper(II) chloride (0.360 mmol) to a 1 mL solution of **Hppy** (0.345 mmol) in DMF, followed by cluster **1** (0.016 mmol) and TEA (0.360 mmol). The lesser molar concentration of copper chloride was used to limit the absorption of photons emitted by europium, as the metallogel possesses a broad absorption band observed from 550 - 800nm (europium emits chiefly at 620 nm).

S2. Crystallographic data

S2.1 Table S2 Crystallographic data for $[\text{CuCl}_2(\text{Hppy})_2]$

Complex	$[\text{CuCl}_2(\text{Hppy})_2]$
Empirical formula	$\text{C}_{16}\text{H}_{14}\text{Cl}_{12}\text{CuN}_6$
Formula weight	424.77
Crystal system	Orthorhombic
Space group	$P\overline{n}nm$
$a/\text{\AA}$	3.7720(8)
$b/\text{\AA}$	10.381(2)
$c/\text{\AA}$	20.876(4)
$\alpha/^\circ$	90
$\beta/^\circ$	90
$\gamma/^\circ$	90
$V/\text{\AA}^3$	817.4(3)
Z	2
$D_c/\text{g cm}^{-3}$	1.726
μ/mm^{-1}	1.675
$F(000)$	430
θ range/ $^\circ$	3.90 to 29.38
R_{int}	0.0727
Final R indices [$I > 2\sigma(I)$]	$R_1 = 0.0635$, $wR_2 = 0.1766$
GOF	1.108

S2.2 Selected bond lengths and angles for $[\text{CuCl}_2(\text{Hppy})_2]$:

Table S3 Selected bond lengths for $[\text{CuCl}_2(\text{Hppy})_2]$

Cu(1)-N(1)	2.004(4)
Cu(1)-N(1)#1	2.004(4)
Cu(1)-Cl(1)	2.3126(12)
Cu(1)-Cl(1)#1	2.3126(12)
C(2)-C(1)	1.382(5)
C(2)-C(3)	1.398(4)
C(3)-C(2)#2	1.398(4)
C(3)-C(4)	1.455(7)
N(1)-C(1)	1.341(4)
N(1)-C(1)#2	1.341(4)
C(4)-C(5)	1.375(6)
C(4)-N(2)#2	1.375(6)
C(4)-C(5)#2	1.375(6)
C(5)-C(6)	1.343(8)
C(6)-C(6)#2	1.405(13)

Table S4 Selected bond angles for **1**

N(1)-Cu(1)-N(1)#1	180.0
N(1)-Cu(1)-Cl(1)	90.0
N(1)#1-Cu(1)-Cl(1)	90.0
N(1)-Cu(1)-Cl(1)#1	90.0
N(1)#1-Cu(1)-Cl(1)#1	90.0
Cl(1)-Cu(1)-Cl(1)#1	180.0
C(1)-C(2)-C(3)	119.8(3)
C(1)-C(2)-H(2)	120.1
C(3)-C(2)-H(2)	120.1
C(2)-C(3)-C(2)#2	116.9(4)
C(2)-C(3)-C(4)	121.6(2)
C(2)#2-C(3)-C(4)	121.6(2)
C(1)-N(1)-C(1)#2	117.8(4)
C(1)-N(1)-Cu(1)	121.1(2)
C(1)#2-N(1)-Cu(1)	121.1(2)
N(1)-C(1)-C(2)	122.9(3)
N(1)-C(1)-H(1)	118.6
C(2)-C(1)-H(1)	118.6
C(5)-C(4)-N(2)#2	112.9(6)
C(5)-C(4)-C(5)#2	112.9(6)
C(5)-C(4)-C(3)	123.5(3)
N(2)#2-C(4)-C(3)	123.5(3)
C(5)#2-C(4)-C(3)	123.5(3)
C(6)-C(5)-C(4)	104.3(6)
C(6)-C(5)-H(5)	127.9
C(4)-C(5)-H(5)	127.9
C(5)-C(6)-C(6)#2	109.3(3)
C(5)-C(6)-H(6)	125.4
C(6)#2-C(6)-H(6)	125.4

S3. Cu(ClO₄)₂ gel

S3.1 SEM image of Cu(ClO₄)₂ gel

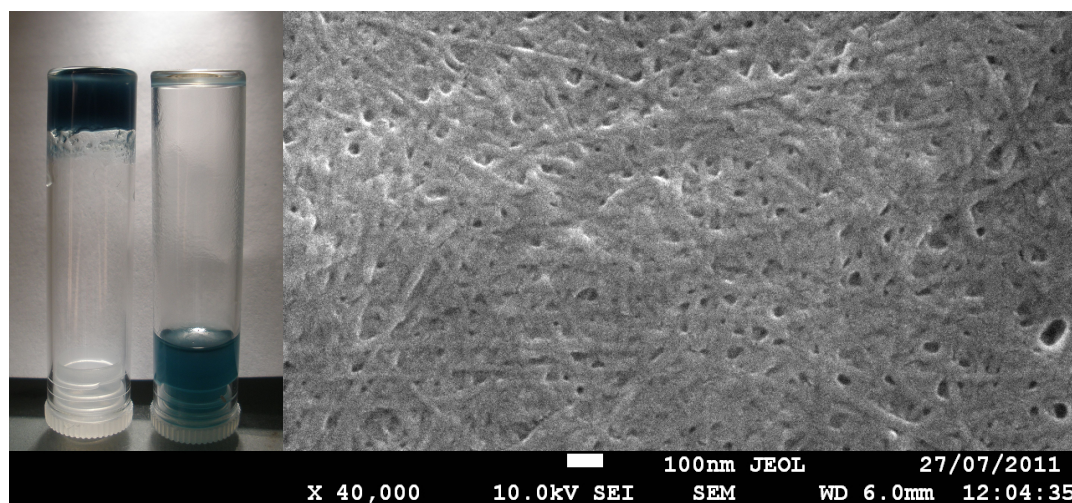


Figure S1 SEM image of the dried perchlorate gel highlighting the thin tape-like morphology. The inset image displays the metallogel next to a DMF solution of the components in the absence of base.

S4. Spectroscopic data

S4.1 Solution IR spectra of ligand, ligand and metal chloride, metallogel¹

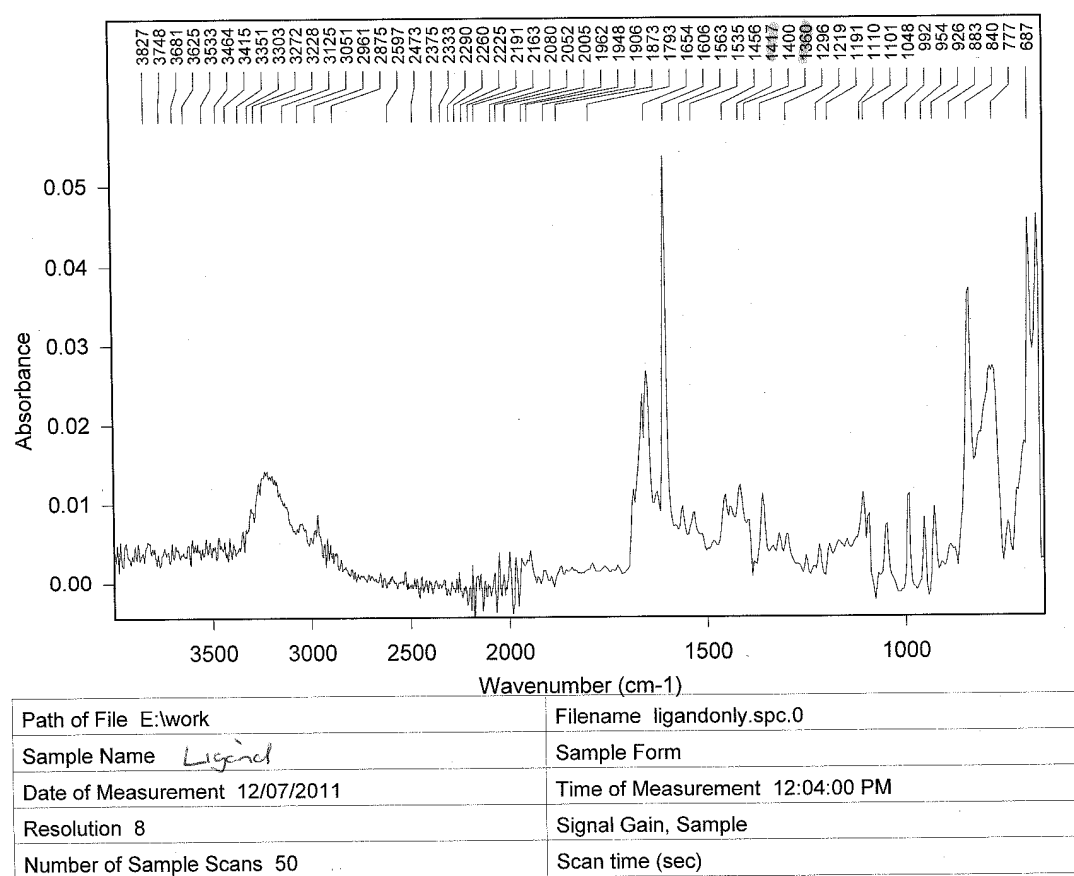


Figure S2 Solution IR of ligand in DMF.

¹ A solvent subtraction has been performed to remove bands associated with dimethylformamide.

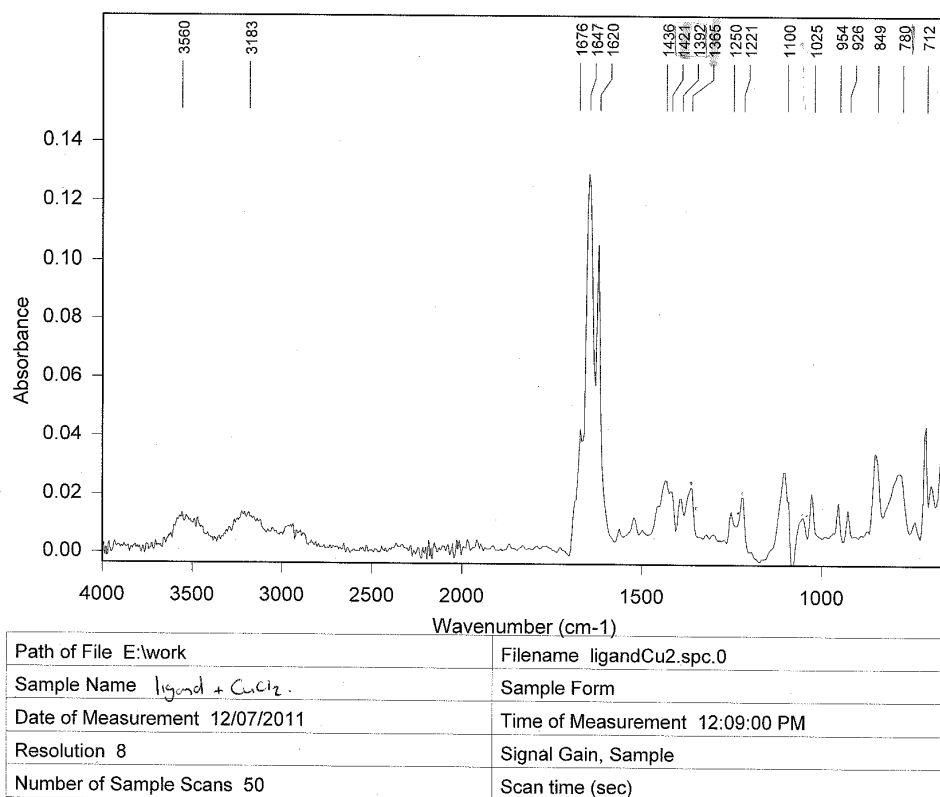


Figure S3 Solution IR of ligand + copper(II) chloride

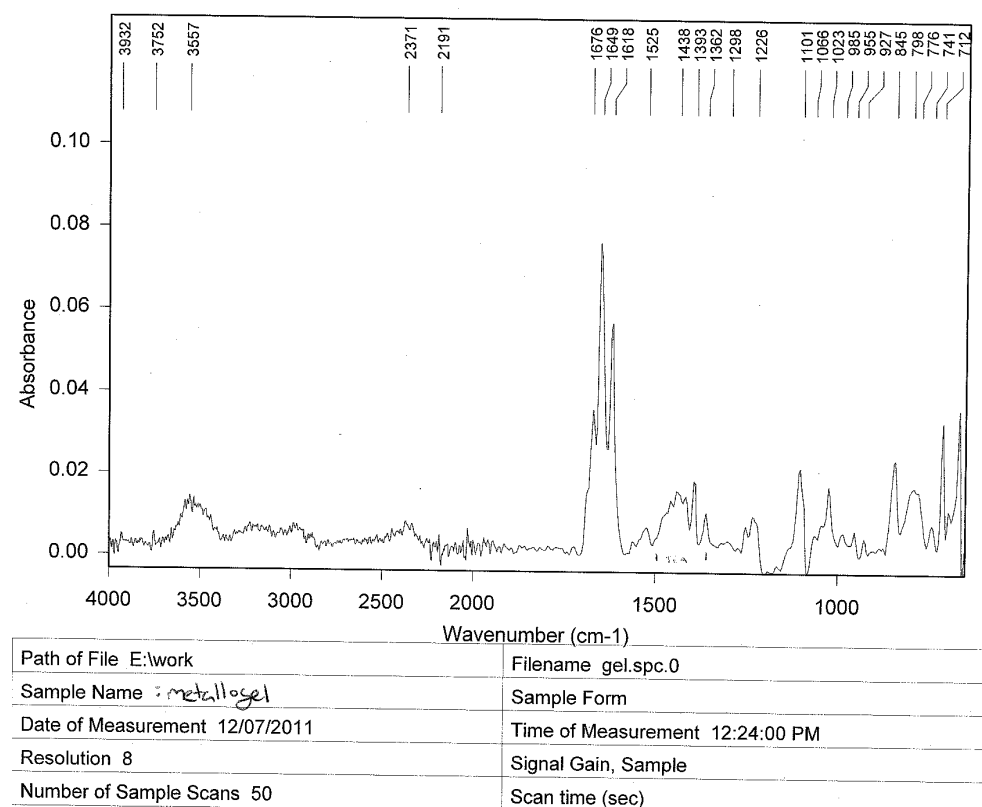
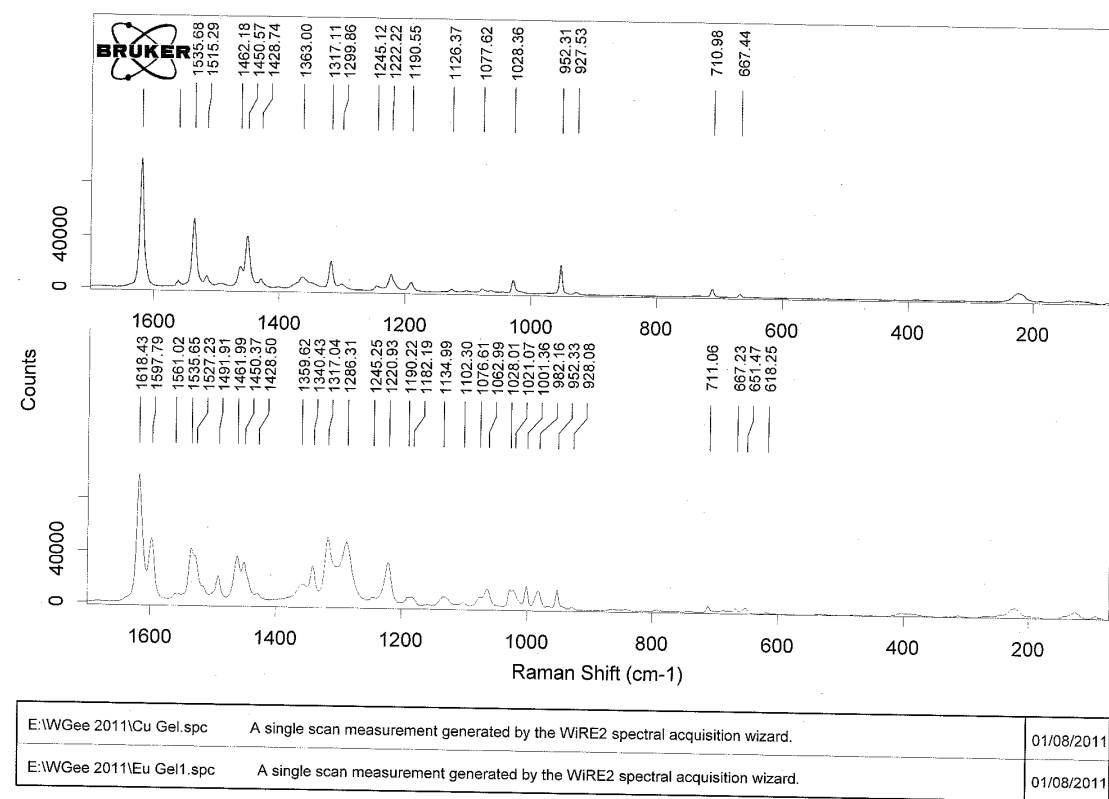


Figure S4 Solution IR of metallogel

S4.2 Raman spectrum of metallogel and metallogel containing **1**



Page 1/1

Figure S5 Comparison between Raman spectra of the metallogel (top) with the metallogel encapsulating europium cluster **1** (bottom).

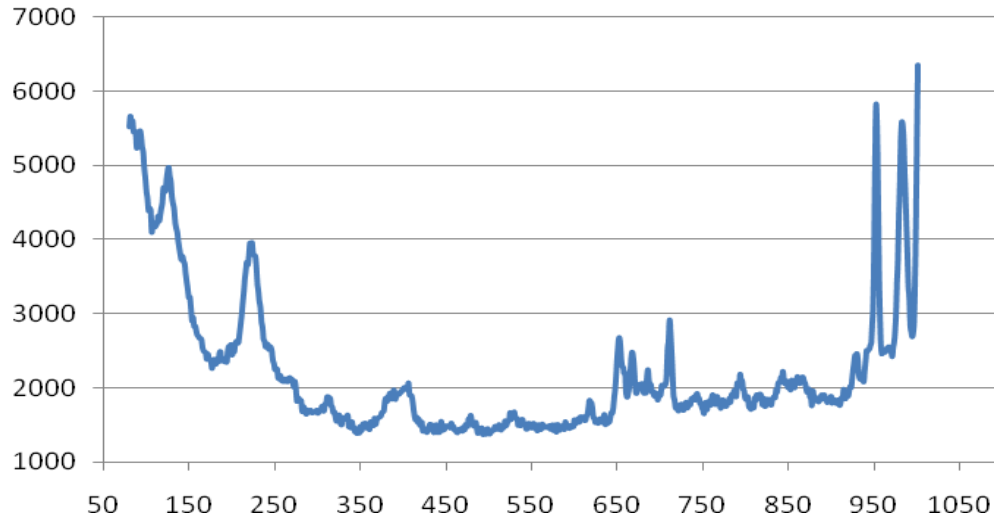


Figure S6 Expansion of the 50 - 1000 wave number region of the Raman spectrum (Figure S5).

S5. Powder XRD data and discussion

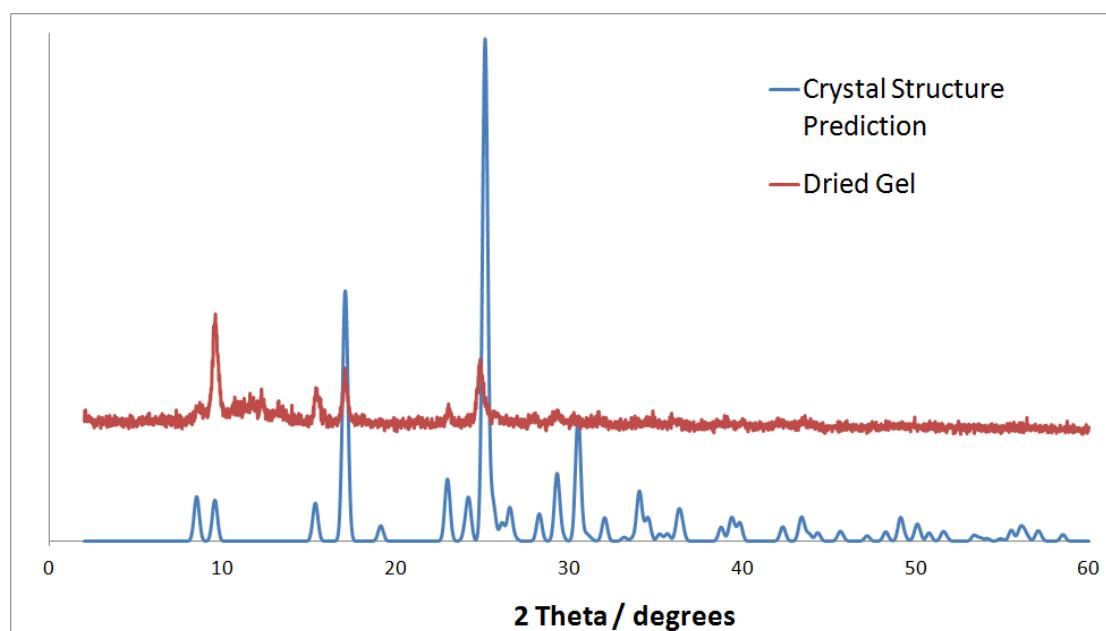


Figure S7 Comparison between the powder X-ray diffraction obtained from the dried metallogel and that predicted from the crystal structure of $[\text{CuCl}_2(\text{Hppy})_2]$.

Dried samples of metallogel **1** and the related perchlorate variant were analysed by powder X-ray diffraction. Of the two, only gel **1** was found to exhibit crystalline character. Overlaying the predicted powder pattern obtained from the structure of $[\text{CuCl}_2(\text{Hppy})_2]$ shows that the bulk of the expected peaks are present, albeit at low intensity.

S6. Titration Curve of Hppy with triethylamine

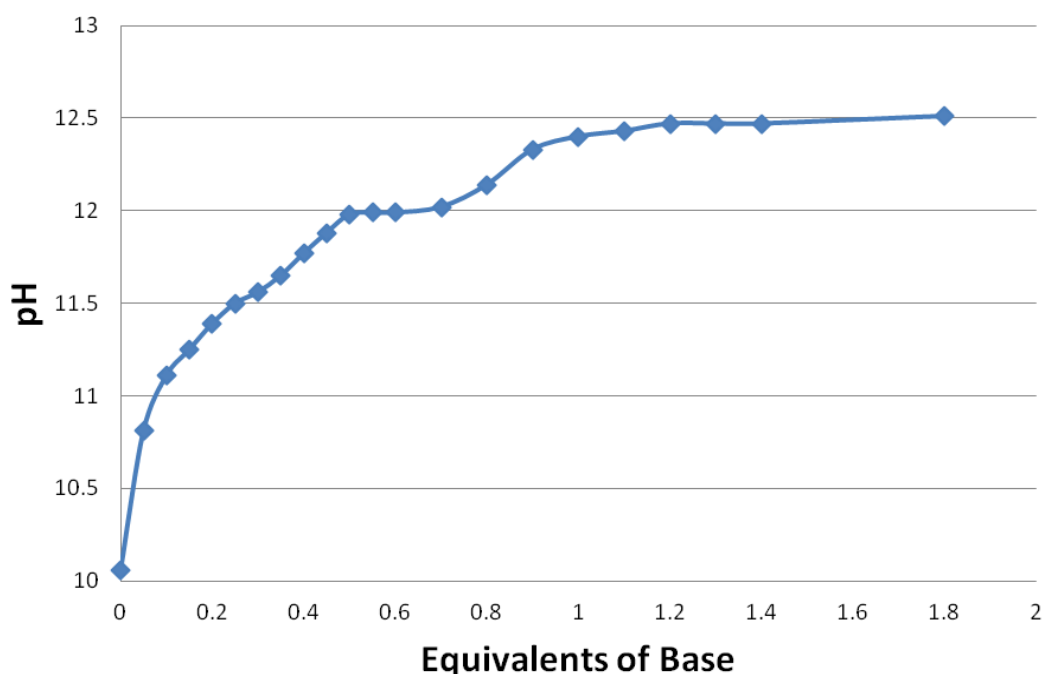


Figure S7 Titration curve of **Hppy** (2 mmol, 0.2 M in DMF) against equivalents of triethylamine.

To justify that triethylamine is able to deprotonate the pyrazole ligand we have performed a titration curve of the pyrazole ligand using triethylamine as the base and DMF as solvent. The pK_a of **Hppy** was determined to be at a pH of 11.98, near to the observed limit of basicity for triethylamine (**tea**) at a pH of approximately 12.5. The initial pH was determined to be 10.06, owing to the basicity of the pyridyl groups. Literature calculations place the pK_a of triethylamine hydrochloride in a solution of DMF at a pH of 10.2.^{S2} A metallogel synthesised according to procedure S1.2. using 10 mL of DMF was next analysed and determined to have a pH of 9.32. The relative proximity of the two pK_a values for protonated triethylamine and the pyrazole ligand suggest that in equilibrium the species can overlap, however at pH 9.32, as determined for the gel, the equilibrium will strongly favour protonated pyrazole

ligand and deprotonated triethylamine. This is consistent with the observation that gellation is initiated by the addition of triethylamine, which likely serves to adhere the 1D chain structures into a gel nanostructure by localised displacements of chloride bridges by the anionic pyrazole groups.

S7. References:

- S1 H. Adams, S. R. Batten, G. M. Davies, M. B. Duriska, J. C. Jeffery, P. Jensen, J. Lu, G. R. Motson, S. J. Coles, M. B. Hursthouse, M. D. Ward. *Dalton Trans.* **2005**, 1910.
- S2 S. S. Kurek, B. J. Laskowska, A. Stokłosa. *Electrochim. Acta*, **2006**, 51, 2306.